Nonlinear Functional Analysis and Applications
Vol. 30, No. 4 (2025), pp. 1053-1081
ISSN: 1229-1595(print), 2466-0973(online)

https://doi.org/10.22771/nfaa.2025.30.04.05
http://nfaa.kyungnam.ac.kr/journal-nfaa

FRACTIONAL-ORDER MODELING OF CO-INFECTION DYNAMICS IN EBOLA AND NIPAH VIRUS TRANSMISSION: A QUALITATIVE AND NUMERICAL ANALYSIS

Dhivya Sundar[1] and Vediyappan Govindan[2]

[1]Department of Mathematics, Hindustan Institute of Technology and Science, Chennai, Tamil Nadu, India
e-mail: dhivyasundar.msc@gmail.com

[2]Department of Mathematics, Hindustan Institute of Technology and Science, Chennai, Tamil Nadu, India
e-mail: vgovindandr@gmail.com

Abstract. This study presents a fractional-order model for EBOV-NIV co-infection dynamics in humans and fruit bats using the Atangana-Baleanu derivative. Fixed-point theory and Hyers-Ulam stability establish existence, uniqueness, and model stability. Fractional-order derivatives outperform integer-order models in capturing memory-dependent transmission. Numerical simulations ($\alpha = 0.99$ vs. 1.0) reveal significant recovery rate influence on co-infection peaks and persistence. The approach aligns with real epidemiological patterns and supports targeted control strategies.

1. Introduction

The Ebola virus (EBOV), part of the Filoviridae family, is notorious for its high mortality rate in both humans and other primates. The severe outbreak of Ebola virus disease in West Africa resulted in over 11,000 deaths [44, 45]. Recently, the virus has frequently spread from animal hosts to humans, with infected individuals remaining contagious, highlighting the persistent risk of outbreaks [18, 22, 27, 31]. Despite some promising developments in clinical trials, no vaccines or treatments for EBOV have been approved yet. This

[0]Received April 12, 2025. Revised June 18, 2025. Accepted June 20, 2025.
[0]2020 Mathematics Subject Classification: 26A33, 34A08.
[0]Keywords: Ebola virus, Nipah virus, co-infection model, fractional calculus, Atangana-Baleanu derivative, stability analysis, numerical simulation.
[0]Corresponding author: V. Govindan(vgovindandr@gmail.com).

emphasizes the urgent need for innovative strategies to combat this dangerous health threat.

In 1998 [24, 26, 37], an outbreak of severe encephalitis and pneumonia among pig farmers and workers in slaughterhouses in Malaysia and Singapore led to the identification of Nipah virus (NIV), a zoonotic paramyxovirus. Since then, NIV has caused numerous outbreaks in the Philippines, Bangladesh, and India, leading to over 600 cases and a fatality rate exceeding 50%. Like EBOV, NIV continues to pose a threat to public health in Southeast Asia, as there are currently no approved vaccines or treatments.

For a long time, ordinary differential equations have been used to model the spread of contagious diseases, helping to understand epidemic transmission patterns. However, the advent of fractional calculus has provided new perspectives on the dynamics of disease transmission. Fractional-order differential equations have become valuable tools for analyzing biological and technical systems, allowing for a more comprehensive understanding of disease transmission dynamics.

The Mittag-Leffler kernel derivative has recently been applied to model various real-world phenomena. After studying the spread of the Q fever epidemic, researchers concluded that trajectories of certain fractional orders converge to a common endemic equilibrium point, unlike integer-order derivatives [15]. Furthermore, the Atangana-Baleanu (A-B) fractional differential operator was found to model disease susceptibility more accurately, requiring fewer infectious individuals. Another study used the Mittag-Leffler kernel to investigate the presence, uniqueness, and stability of HIV/AIDS infection models [16]. Similarly, a separate study [12] examined the kinetics of COVID-19, emphasizing the importance of memory in its transmission, while Okyere et al. [34] analyzed a SIR model based on the Caputo derivative.

Berge et al. [17] developed an infected-recovered-death model with natural mortality in SIR compartments to study the transmission of Ebola virus disease in sub-Saharan Africa. Omeloye-Adewale [35] conducted a mathematical analysis of the transmission dynamics of Ebola malaria. Biswas [19] explored the dynamics of NIV using an SIR model and examined control and prevention strategies through optimal control techniques ([20],[21],[23],[30],[38],[39],[40]).

Abbas [4] investigated relationships arising from a generalized form of the Prabhakhar fractional derivative. The application of the Caputo-Fabrizio model to fluid flow in the unsteady boundary layer of a Casson fluid was discussed [2, 3]. Abbas [1, 5, 6] showed how the Laplace transform method is employed to solve dimensionless partial differential equations and obtain solutions. Another study [42] explored an epidemic model that describes the deterministic influence of media coverage on the transmission of COVID-19.

Mondal et al. [32] studied predator-prey dynamics, applying a generalized predator-prey model [41].

Khan [28] established results for existence and H-U stability using fixed-point theory. Changdev et al. [25] studied the basic solution of the Dirichlet problem with first derivative constant conditions. Pakhira [36] emphasized the importance of sensitive parameters, especially the strong memory effect. Abdelhakem [10] used polynomial boundary techniques, which are well-known in Legendre basic functions [7, 8, 9]. Several methods for approximating solutions to ordinary differential equations, such as the Adams-Bashforth-Moulton and Runge-Kutta methods, are discussed [13].

The Atangana-Baleanu-Caputo (ABC) derivative has shown exceptional ability in modeling memory effects and long-range dependence in epidemiological processes. From the literature, it is evident that separate models for the transmission dynamics of Nipah and Ebola viruses have been analyzed both qualitatively and numerically. In this study, we present a new and more efficient mathematical model for the dynamics of Ebola and Nipah virus co-infection. To the best of our knowledge, no prior work has specifically addressed co-infection dynamics using U-H type results.

Fractional differential equations play a crucial role in modeling anomalous relaxation and diffusion processes. The convolution integral introduced by fractional derivatives, which includes a power-law memory, makes fractional differential equations essential for describing memory effects in complex systems. Fractional calculus approaches within mathematically informed frameworks provide a deeper understanding of complex processes, offering novel models applicable to optimization methods. In computer science, fractional calculus is used to analyze algorithms, aiding in the evaluation of computational difficulty and resource requirements.

This research bridges epidemiology, mathematics, and computational science, demonstrating its interdisciplinary nature. In our study, we explore the co-infection dynamics of the Nipah and Ebola viruses by using fractional-order derivatives, establishing connections between mathematical theory and biological systems. This approach, which mimics brain-like computation and scaling behaviors, enhances our understanding of epidemiology and complex systems, especially concerning the interactions between various viral dynamics and their effects on host species like fruit bats and humans.

In this paper, we present a co-infection model for EBOV-NIV using a three-compartment (SIR) framework that incorporates the A-B fractional derivative. We examine the existence and singularity of solutions, investigate H-U stability, and perform numerical simulations based on specific assumptions for the

model parameters. This work contributes to a deeper understanding of co-infection dynamics and offers valuable insights into potential control measures for these dangerous viruses.

(i) The use of the A-B derivative may offer novel insights into the co-dynamics of Ebola and Nipah viruses.
(ii) We analyze the existence and uniqueness of the proposed co-dynamics model for Ebola and Nipah viruses using the Atangana-Baleanu derivative. By applying the fixed point theorem, this research enhances our understanding of these viruses' dynamics and potential control measures.
(iii) By utilizing the generalized M-L kernel, we demonstrate the co-dynamics of Ebola and Nipah viruses. Through simulations, we account for various factors that influence disease spread and impact, aiding in the development of effective control strategies.
(iv) In our study of the co-infection dynamics of EBOV and NIV, we highlight the significant impact of the recovery rate. We specifically examine how this parameter influences co-infection dynamics when using a fractional order of 0.99 as opposed to the integer order of 1. This distinction underscores the role of fractional calculus in understanding disease transmission and provides crucial insights for effective disease management and control.

The remainder of the paper is organized as follows: Section 2 introduces fundamental concepts and initial results. In Section 3, we present the Ebola-Nipah co-infection model along with the relevant parameters. Sections 4 and 5 discuss the H-U stability and existence of solutions for the proposed model. Section 6 presents numerical simulations, and Section 7 concludes with a summary and suggestions for future research.

2. Basic concepts

The study of fractional differential equations spans multiple disciplines and finds applications across a variety of fields, including control systems, heat transfer, biomathematics, complex systems, biomedicine, and financial systems, among others. The Atangana-Baleanu fractional derivatives are particularly favored due to their non-local characteristics, which allow them to more effectively represent complex behaviors compared to traditional operators. In these frameworks, it can be assumed that the observed behavior is contingent upon the order of the fractional derivative model and the transmission rate.

Definition 2.1. ([39]) The fractional Atangana-Baleanu derivative of a function $\phi \in \chi^*(e, f)$, where $f > e$, in the Liouville-Caputo sense for $\beta \in [0, 1]$ is

defined as follows:

$$ {}^{ABC}_{e}D^{\beta}_{\xi}\phi(\xi) = \frac{B(\beta)}{1-\beta}\int_{e}^{\xi}\phi'(s)E_{\beta}\left[\frac{-\beta(\xi-S)^{\beta}}{1-\beta}\right]ds, \tag{2.1} $$

where $B(\beta)$ satisfies $B(0) = B(1) = 1$.

Definition 2.2. ([33]) The Riemann-Liouville interpretation of the fractional AB derivative for a function $\phi \in \chi^{*}(e,f), f > e$, with $\beta \in [0,1]$ is expressed as follows

$$ {}^{ABC}_{e}D^{\beta}_{\xi}\phi(\xi) = \frac{B(\beta)}{1-\beta}\frac{d}{d\xi}\int_{e}^{\xi}\phi'(s)E_{\beta}\left[\frac{-\beta(\xi-S)^{\beta}}{1-\beta}\right]ds. $$

Definition 2.3. ([29]) The Atangana-Baleanu (AB) integral for a function $\phi \in \chi^{*}(e,f), f > e$, when $0 < \beta < 1$, is provided by Gakkhar and Chavda as follows

$$ {}^{AB}_{e}I^{\beta}_{\xi}\phi(\xi) = \frac{1-\beta}{B(\beta)}\phi(\xi) + \frac{\beta}{B(\beta)\Gamma(\beta)}\int_{e}^{\xi}\phi(s)(\xi-s)^{\beta-1}ds. $$

Lemma 2.4. ([11]) *The Newton-Leibniz formula, as discussed by Agarwal-Singh, is applicable to both the AB fractional derivative and the AB fractional integral of the function ϕ,*

$$ {}^{AB}_{e}I^{\beta}_{\xi}\left({}^{ABC}_{e}D^{\beta}_{\xi}\phi(\xi)\right) = \phi(\xi) - \phi(e). $$

Theorem 2.5. ([11]) *For two functions $\phi, \nu \in \wedge'(e,f)$, $f > e$, the ABC and ABR fractional derivatives satisfy the following relationships:*

$$ \|{}^{ABC}_{e}D^{\beta}_{\xi}\phi(\xi) - {}^{ABC}_{e}D^{\beta}_{\xi}\nu(\xi)\| \leq \wedge\|\phi(\xi) - \nu(\xi)\|, $$

$$ \|{}^{ABR}_{e}D^{\beta}_{\xi}\phi(\xi) - {}^{ABR}_{e}D^{\beta}_{\xi}\nu(\xi)\| \leq \wedge\|\phi(\xi) - \nu(\xi)\|. $$

3. EBOV/NIV co-infection model

The results reveal various scaling patterns and fractal dimensions in the dynamics of co-infection involving the Nipah and Ebola viruses. Our model sheds light on how these viruses interact within host populations by identifying critical thresholds and stability regions. These insights extend beyond epidemiology, impacting biology, economics, and human behavior. The interdisciplinary nature of our research illustrates how mathematical and computational methodologies can uncover hidden relationships and guide public health strategies, emphasizing the importance of our study in understanding complex systems. By mapping the behavior of these viruses across different contexts,

our research enhances the understanding of intricate interactions that span multiple domains.

In this section, we present a co-infection model that incorporates both Ebola and Nipah viruses, utilizing the Atangana-Baleanu approach in the Caputo fractional derivative framework. This model draws inspiration from compartmental epidemiological frameworks that have been vital in clarifying the dynamics of epidemic spread and the various strategies employed for their prevention. The model suggests specific sub-populations within the human population, $\mathfrak{N}_H$, which include individuals susceptible to Ebola alone, represented as $\mathfrak{I}_E$, those infected solely with Nipah, denoted as $\mathfrak{I}_N$, individuals co-infected with both viruses, represented as $\mathfrak{I}_{NE}$, and those who have recovered, labeled as $\mathfrak{R}$.

The following is a schematic diagram of the co-infected model under Fig. 1.

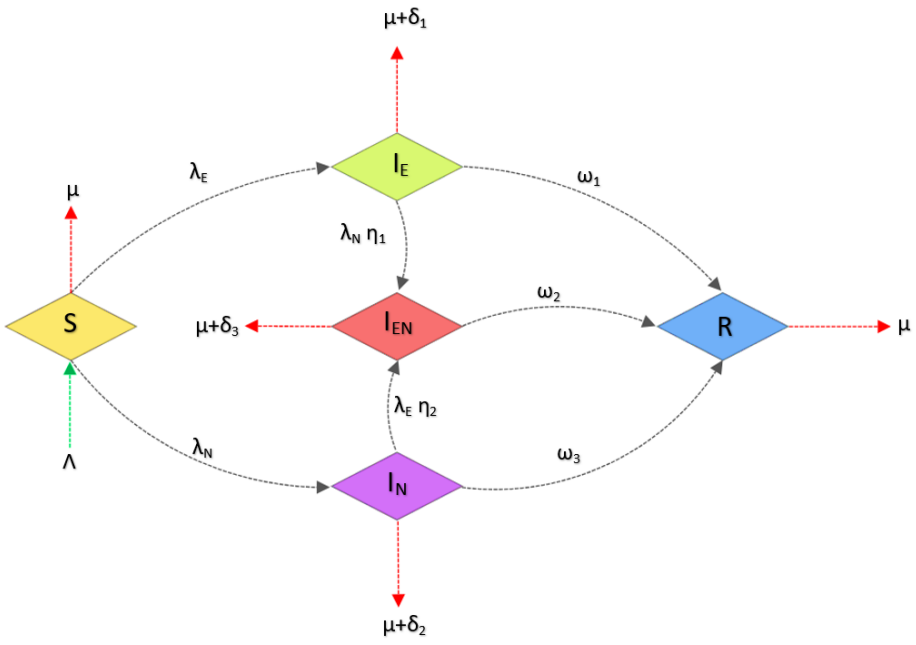

FIGURE 1. Flow-chart of Ebola and Nipah co-infection

Parameters	Description
$\wedge$	Rate of population recruitment
λ_E	Rate at which Ebola is transmitted
λ_N	Rate at which Nipah is transmitted
δ_1	Mortality rate associated with Ebola
δ_2	Mortality rate associated with Nipah
δ_3	Mortality rate due to co-infection from both viruses
ω_1	Rate of recovery from Ebola
ω_2	Rate of recovery from Nipah
ω_3	Rate of recovery from both infections
η_1	Level of latency for Ebola-infected individuals becoming asymptotically infected with Nipah
η_2	Rate of susceptibility of Nipah-infected individuals to Ebola
μ	Natural mortality rate

We assumed that the recruitment process increases the susceptible population at a rate denoted by $\wedge$. Each segment of the population within all compartments undergoes a natural mortality rate of μ.

The infection force λ_E signifies how individuals become susceptible to contracting Ebola; here, β_E represents the effective contact rate associated with Ebola transmission. Meanwhile, the term β_N reflects the effective contact rate for individuals infected with Nipah within the infected compartment ($\mathfrak{I}_E$) of Ebola-infected individuals. In a similar manner, susceptible individuals can contract Nipah via a force of infection λ_N, with the remaining individuals either transitioning to the co-infection compartment ($\mathfrak{I}_{NE}$) at a rate of $\lambda_N\eta_1$ or succumbing to causes related to Ebola at a rate δ_1.

In parallel, those in the Nipah-infected compartment ($\mathfrak{I}_N$) recover from the illness at a recovery rate of ω_2, while others either perish at a rate δ_2 or shift to the co-infection compartment ($\mathfrak{I}_{NE}$) at a rate of $\lambda_E\eta_2$.

Participants in the co-infected compartment ($\mathfrak{I}_{NE}$) are subject to a force of infection represented by $\eta_2\lambda_E$ and $\eta_1\lambda_N$. Portions of these individuals recover at a rate ω_3 or may die due to the combined effects of Ebola and Nipah infection at a rate δ_3.

$$\begin{aligned}
{}_0^{ABC}D_\xi^{\beta_1}\mathfrak{S}_H(\xi) &= \wedge - (\lambda_E + \lambda_N + \mu)\mathfrak{S},\\
{}_0^{ABC}D_\xi^{\beta_2}\mathfrak{I}_E(\xi) &= \lambda_E\mathfrak{S} - (\mu + \delta_1 + \lambda_N\eta_1 + \omega_1)\mathfrak{I}_E,\\
{}_0^{ABC}D_\xi^{\beta_3}\mathfrak{I}_{NE}(\xi) &= \lambda_N\eta_1\mathfrak{I}_E + \lambda_E\eta_2\mathfrak{I}_N - (\mu + \delta_3 + \omega_2)\mathfrak{I}_{NE},\\
{}_0^{ABC}D_\xi^{\beta_4}\mathfrak{I}_N(\xi) &= \lambda_N\mathfrak{S} - (\mu + \delta_2 + \lambda_E\eta_2 + \omega_3)\mathfrak{I}_N,
\end{aligned} \tag{3.1}$$

$$ {}_{0}^{ABC}D_{\xi}^{\beta_5}\mathfrak{R}(\xi) = \omega_1\mathfrak{I}_E + \omega_2\mathfrak{I}_{NE} + \omega_3\mathfrak{I}_N - \mu\mathfrak{R}, $$

where

$$ \lambda_E = \frac{\beta_E(\mathfrak{I}_E + \mathfrak{I}_{EN})}{N}, $$
$$ \lambda_N = \frac{\beta_N(\mathfrak{I}_N + \mathfrak{I}_{EN})}{N} $$

and

$$ N(\xi) = \mathfrak{S}_H + \mathfrak{I}_E + \mathfrak{I}_{NE} + \mathfrak{I}_N + \mathfrak{R}. $$

The initial conditions of Ebola and Nipah co-infection model become: $\mathfrak{S}_H(0) = \mathfrak{S}_0(\xi)$, $\mathfrak{I}_E(0) = \mathfrak{I}_0^E(\xi)$, $\mathfrak{I}_{NE}(0) = \mathfrak{I}_0^{NE}(\xi)$, $\mathfrak{I}_N(0) = \mathfrak{I}_0^N(\xi)$, $\mathfrak{R}(0) = \mathfrak{R}_0(\xi)$.

4. Existence and uniqueness of the solution

This section investigates the existence of a solution for the fractional order EBOV/NIV model 3 through fixed point approaches

$$ \begin{aligned} \mathfrak{S}(\xi) - \mathfrak{S}(0) = {} & \frac{1-\beta_1}{B(\beta_1)}\left(\wedge - \frac{\beta_E(\mathfrak{I}_E + \mathfrak{I}_{NE})}{N} + \frac{\beta_N(\mathfrak{I}_N + \mathfrak{I}_{NE})}{N} + \mu\right)\mathfrak{S} \\ & + \frac{\beta_1}{B(\beta_1)\Gamma(\beta_1)}\int_0^{\xi}(\xi - s)^{\beta_1 - 1} \\ & \times \left[\wedge - \frac{\beta_E(\mathfrak{I}_E + \mathfrak{I}_{NE})}{N} + \frac{\beta_N(\mathfrak{I}_N + \mathfrak{I}_{NE})}{N} + \mu\right]\mathfrak{S}ds, \end{aligned} $$

$$ \begin{aligned} \mathfrak{I}_E(\xi) - \mathfrak{I}_E(0) = {} & \frac{1-\beta_2}{B(\beta_2)}\left(\lambda_E\mathfrak{S} - (\mu + \delta_1 + \lambda_N\eta_1 + \omega_1)\mathfrak{I}_E\right) \\ & + \frac{\beta_2}{B(\beta_2)\Gamma(\beta_2)}\int_0^{\xi}(\xi - s)^{\beta_2 - 1} \\ & \times \left[\lambda_E\mathfrak{S} - (\mu + \delta_1 + \lambda_N\eta_1 + \omega_1)\mathfrak{I}_E\right]ds, \end{aligned} $$

$$ \begin{aligned} \mathfrak{I}_{NE}(\xi) - \mathfrak{I}_{NE}(0) = {} & \frac{1-\beta_3}{B(\beta_3)}\left(\lambda_N\eta_1\mathfrak{I}_E + \lambda_E\eta_2\mathfrak{I}_N - (\mu + \delta_3 + \omega_2)\mathfrak{I}_{NE}\right) \\ & + \frac{\beta_3}{B(\beta_3)\Gamma(\beta_3)}\int_0^{\xi}(\xi - s)^{\beta_3 - 1} \\ & \times \left[\lambda_N\eta_1\mathfrak{I}_E + \lambda_E\eta_2\mathfrak{I}_N - (\mu + \delta_3 + \omega_2)\mathfrak{I}_{NE}\right]ds, \end{aligned} $$

$$ \begin{aligned} \mathfrak{I}_N(\xi) - \mathfrak{I}_N(0) = {} & \frac{1-\beta_4}{B(\beta_4)}\left(\lambda_N\mathfrak{S} + (\mu + \delta_2 + \lambda_E\eta_2 + \omega_3)\mathfrak{I}_N\right) \\ & + \frac{\beta_4}{B(\beta_4)\Gamma(\beta_4)}\int_0^{\xi}(\xi - s)^{\beta_4 - 1} \end{aligned} $$

$$\times \left[\lambda_N \mathfrak{S} + (\mu + \delta_2 + \lambda_E \eta_2 + \omega_3)\mathfrak{I}_N\right] ds,$$

$$\mathfrak{R}(\xi) - \mathfrak{R}(0) = \frac{1-\beta_5}{B(\beta_5)}\left(\omega_1 \mathfrak{I}_E + \omega_2 \mathfrak{I}_{NE} + \omega_3 \mathfrak{I}_N - \mu \mathfrak{R}\right) + \frac{\beta_5}{B(\beta_5)\Gamma(\beta_5)} \int_0^{\xi} (\xi - s)^{\beta_5 - 1} \left[\omega_1 \mathfrak{I}_E + \omega_2 \mathfrak{I}_{NE} + \omega_3 \mathfrak{I}_N - \mu \mathfrak{R}\right] ds. \tag{4.1}$$

To keep things simple, we create the functions K_i, and a few constants ϕ_i, where $i \in N_1^5$,

$$K_1(\xi, \mathfrak{S}) = \wedge - \left[(\mathfrak{I}_E + \mathfrak{I}_{EN})\frac{\beta_E}{N} + (\mathfrak{I}_N + \mathfrak{I}_{NE})\frac{\beta_N}{N} + \mu\right] \mathfrak{S}, \tag{4.2}$$

$$K_2(\xi, \mathfrak{I}_E) = (\mathfrak{I}_E + \mathfrak{I}_{EN})\frac{\beta_E}{N}\mathfrak{S} - \left(\mu + \delta_1 + (\mathfrak{I}_N + \mathfrak{I}_{NE})\frac{\beta_N}{N} + \eta_1 + \omega_1\right) \mathfrak{I}_E, \tag{4.3}$$

$$K_3(\xi, \mathfrak{I}_{NE}) = (\mathfrak{I}_N + \mathfrak{I}_{NE})\frac{\beta_N}{N}\eta_1 \mathfrak{I}_E + (\mathfrak{I}_E + \mathfrak{I}_{NE})\frac{\beta_E}{N}\eta_2 \mathfrak{I}_N - (\mu + \delta_3 + \omega_2)\mathfrak{I}_{NE}, \tag{4.4}$$

$$K_4(\xi, \mathfrak{I}_N) = (\mathfrak{I}_N + \mathfrak{I}_{NE})\frac{\beta_N}{N}\mathfrak{S} - \left(\mu + s_2 + (\mathfrak{I}_E + \mathfrak{I}_{NE})\frac{\beta_E}{N}\eta_2 + \omega_3\right) \mathfrak{I}_N, \tag{4.5}$$

$$K_5(\xi, \mathfrak{R}) = \omega_1 \mathfrak{I}_E + \omega_2 \mathfrak{I}_{NE} + \omega_3 \mathfrak{I}_N - \mu \mathfrak{R}. \tag{4.6}$$

Theorem 4.1. *Under assumption B, the kernels K_i for $i \in N_1^5$ satisfy the Lipschitz condition and act as contractions whenever $\phi_i < 1$ for each $i \in N_1^5$.*

Proof. To begin, we show that the Lipschitz condition holds for $K_1(\xi, \mathfrak{S})$. Evaluating equation (4.2) for $\mathfrak{S}(\xi)$ and $\mathfrak{S}^*(\xi)$ gives

$$\begin{aligned}
\|K_1(\xi, \mathfrak{S}) - K_1(\xi, \mathfrak{S}^*)\| &= \| \wedge - \left[(\mathfrak{I}_E + \mathfrak{I}_{NE})\frac{\beta_E}{N} + (\mathfrak{I}_N + \mathfrak{I}_{NE})\frac{\beta_N}{N} + \mu\right] \mathfrak{S} \\
&\quad - \left(\wedge - (\mathfrak{I}_E + \mathfrak{I}_{NE})\frac{\beta_E}{N} + (\mathfrak{I}_N + \mathfrak{I}_{NE})\frac{\beta_N}{N} + \mu\right) \mathfrak{S}^* \| \\
&\leq \left[(\mathfrak{I}_E + \mathfrak{I}_{NE})\frac{\beta_E}{N} + (\mathfrak{I}_N + \mathfrak{I}_{NE})\frac{\beta_N}{N} + \mu\right] \|\mathfrak{S} - \mathfrak{S}^*\| \\
&\leq [\lambda_E + \lambda_N + \mu] \|\mathfrak{S} - \mathfrak{S}^*\| \\
&\leq \phi_1 \|\mathfrak{S} - \mathfrak{S}^*\|.
\end{aligned} \tag{4.7}$$

Similarly, we have

$$\|K_2(\xi, \mathfrak{I}_E) - K_2(\xi, \mathfrak{I}_E^*)\| \leq \phi_2 \|\mathfrak{I}_E - \mathfrak{I}_E^*\|, \tag{4.8}$$

$$\|K_3(\xi, \mathfrak{I}_{NE}) - K_2(\xi, \mathfrak{I}_{NE}^*)\| \leq \phi_3 \|\mathfrak{I}_{NE} - \mathfrak{I}_{NE}^*\|, \tag{4.9}$$

$$\|K_4(\xi, \mathfrak{I}^*_{NE})\| \leq \phi_4 \|\mathfrak{I}_N - \mathfrak{I}^*_N\|, \tag{4.10}$$

$$\|K_5(\xi, \mathfrak{R}) - K_5(\xi, \mathfrak{R}^*)\| \leq \phi_5 \|\mathfrak{R} - \mathfrak{R}^*\|. \tag{4.11}$$

The kernels K_i, $i \in N_1^5$ are thus contractions with $\phi_i < 1$, $i \in N_1^5$, and therefore fulfill the Lipschitz condition. The proof is now complete. □

By Using the kernels K_i, $i \in N_1^5$ and initial states $\mathfrak{S}(0) = \mathfrak{I}_E(0) = \mathfrak{I}_N(0) = \mathfrak{I}_{NE}(0) = \mathfrak{R}(0) = 0$. The system represented by equation (4.3) is rewritten as follows:

$$\mathfrak{S}(\xi) = \frac{1-\beta_1}{B(\beta_1)} K_1(\xi, \mathfrak{S}(\xi)) + \frac{\beta_1}{B(\beta_1)\Gamma(\beta_1)} \int_0^\xi (\xi - s)^{\beta_1 - 1} K_1(s, \mathfrak{S}(s)) ds, \tag{4.12}$$

$$\mathfrak{I}_E(\xi) = \frac{1-\beta_2}{B(\beta_2)} K_2(\xi, \mathfrak{I}_E(\xi)) + \frac{\beta_2}{B(\beta_2)\Gamma(\beta_2)} \int_0^\xi (\xi - s)^{\beta_2 - 1} K_2(s, \mathfrak{I}_E(s)) ds, \tag{4.13}$$

$$\mathfrak{I}_{NE}(\xi) = \frac{1-\beta_3}{B(\beta_3)} K_3(\xi, \mathfrak{I}_{NE}(\xi)) + \frac{\beta_3}{B(\beta_3)\Gamma(\beta_3)} \int_0^\xi (\xi - s)^{\beta_3 - 1} K_3(s, \mathfrak{I}_{NE}(s)) ds, \tag{4.14}$$

$$\mathfrak{I}_N(\xi) = \frac{1-\beta_4}{B(\beta_4)} K_4(\xi, \mathfrak{I}_N(\xi)) + \frac{\beta_4}{B(\beta_4)\Gamma(\beta_4)} \int_0^\xi (\xi - s)^{\beta_4 - 1} K_4(s, \mathfrak{I}_N(s)) ds, \tag{4.15}$$

$$\mathfrak{R}(\xi) = \frac{1-\beta_5}{B(\beta_5)} K_5(\xi, \mathfrak{R}(\xi)) + \frac{\beta_5}{B(\beta_5)\Gamma(\beta_5)} \int_0^\xi (\xi - s)^{\beta_5 - 1} K_5(s, \mathfrak{R}(s)) ds. \tag{4.16}$$

Now, we define the following recursive formulas:

$$\begin{aligned} \mathfrak{S}_n(\xi) = {} & \frac{1-\beta_1}{B(\beta_1)} K_1(t, \mathfrak{S}_{n-1}(\xi)) \\ & + \frac{\beta_1}{B(\beta_1)\Gamma(\beta_1)} \int_0^\xi (\xi - s)^{\beta_1 - 1} K_1(s, \mathfrak{S}_{n-1}(s)) ds, \end{aligned} \tag{4.17}$$

$$\begin{aligned} \mathfrak{I}_{En}(\xi) = {} & \frac{1-\beta_2}{B(\beta_2)} K_2(\xi, \mathfrak{I}_{En-1}(\xi)) \\ & + \frac{\beta_2}{B(\beta_2)\Gamma(\beta_2)} \int_0^\xi (\xi - s)^{\beta_2 - 1} K_2(s, \mathfrak{I}_{En-1}(s)) ds, \end{aligned} \tag{4.18}$$

$$\begin{aligned} \mathfrak{I}_{NE_n}(\xi) = {} & \frac{1-\beta_3}{B(\beta_3)} K_3(\xi, \mathfrak{I}_{NE_{n-1}}(\xi)) \\ & + \frac{\beta_3}{B(\beta_3)\Gamma(\beta_3)} \int_0^\xi (\xi - s)^{\beta_3 - 1} K_3(s, \mathfrak{I}_{NE_{n-1}}(s)) ds, \end{aligned} \tag{4.19}$$

$$\mathfrak{I}_{N_n}(\xi) = \frac{1-\beta_4}{B(\beta_4)} K_4(\xi, \mathfrak{I}_{N_{n-1}}(\xi))$$

$$+\frac{\beta_4}{B(\beta_4)\Gamma(\beta_4)}\int_0^{\xi}(\xi-s)^{\beta_4-1}K_4(s,\mathfrak{I}_{N_{n-1}}(s))ds, \tag{4.20}$$

$$\mathfrak{R}_n(\xi)=\frac{1-\beta_5}{B(\beta_5)}K_5(\xi,\mathfrak{R}_{n-1}(\xi))$$
$$+\frac{\beta_5}{B(\beta_5)\Gamma(\beta_5)}\int_0^{\xi}(\xi-s)^{\beta_5-1}K_5(s,\mathfrak{R}_{n-1}(s))ds. \tag{4.21}$$

Consider the differences,

$$G\mathfrak{S}_{n+1}(\xi)=(\mathfrak{S}_{n+1}-\mathfrak{S}_n)(\xi)$$
$$=\frac{1-\beta_1}{B(\beta_1)}\left(K_1(\xi,\mathfrak{S}_n(\xi))-K_1(\xi,\mathfrak{S}_{n-1}(\xi))\right)$$
$$+\frac{\beta_1}{B(\beta_1)\Gamma(\beta_1)}\int_0^{\xi}(\xi-s)^{\beta_1-1}(k_1(s,\mathfrak{S}_n(s))-k_1(s,\mathfrak{S}_{n-1}(s)))ds, \tag{4.22}$$

$$G\mathfrak{I}_{H_{n+1}}(\xi)=(\mathfrak{I}_{H_{n+1}}-\mathfrak{I}_{H_n})(\xi)$$
$$=\frac{1-\beta_2}{B(\beta_2)}\left(K_2(\xi,\mathfrak{I}_{H_n}(\xi))-K_2(\xi,\mathfrak{I}_{H_{n-1}}(\xi))\right)$$
$$+\frac{\beta_2}{B(\beta_2)\Gamma(\beta_2)}\int_0^{\xi}(\xi-s)^{\beta_2-1}(k_2(s,\mathfrak{I}_{H_n}(s))-k_2(s,\mathfrak{I}_{H_{n-1}}(s)))ds, \tag{4.23}$$

$$G\mathfrak{I}_{NE_{n+1}}(\xi)=(\mathfrak{I}_{NE_{n+1}}-\mathfrak{I}_{NE_n})(\xi)$$
$$=\frac{1-\beta_3}{B(\beta_3)}\left(K_3(\xi,\mathfrak{I}_{NE_n}(\xi))-K_3(\xi,\mathfrak{I}_{NE_{n-1}}(\xi))\right)$$
$$+\frac{\beta_3}{B(\beta_3)\Gamma(\beta_3)}\int_0^{\xi}(\xi-s)^{\beta_3-1}(K_3(s,\mathfrak{I}_{NE_n}(s))-k_3(s,\mathfrak{I}_{NE_{n-1}}(s)))ds, \tag{4.24}$$

$$G\mathfrak{I}_{N_{n+1}}(\xi)=(\mathfrak{I}_{N_{n+1}}-\mathfrak{I}_{N_n})(\xi)$$
$$=\frac{1-\beta_4}{B(\beta_4)}\left(K_4(\xi,\mathfrak{I}_{N_n}(\xi))-K_4(\xi,\mathfrak{I}_{H_{n-1}}(\xi))\right)$$
$$+\frac{\beta_4}{B(\beta_4)\Gamma(\beta_4)}\int_0^{\xi}(\xi-s)^{\beta_4-1}(K_4(s,\mathfrak{I}_{N_n}(s))-k_4(s,\mathfrak{I}_{N_{n-1}}(s)))ds, \tag{4.25}$$

$$G\mathfrak{R}_{n+1}(\xi)=(\mathfrak{R}_{n+1}-\mathfrak{R}_n)(\xi)$$
$$=\frac{1-\beta_5}{B(\beta_5)}\left(K_5(\xi,\mathfrak{R}_n(\xi))-K_5(\xi,\mathfrak{R}_{n-1}(\xi))\right)$$
$$+\frac{\beta_5}{B(\beta_5)\Gamma(\beta_5)}\int_0^{\xi}(\xi-s)^{\beta_5-1}(k_5(s,\mathfrak{R}_n(s))-k_5(s,\mathfrak{R}_{n-1}(s)))ds, \tag{4.26}$$

$$\begin{aligned}\|G\mathfrak{S}_{n+1}(\xi)\| &= \|\mathfrak{S}_{n+1}-\mathfrak{S}_n\|(\xi)\\ &= \frac{1-\beta_1}{B(\beta_1)}\|K_1(\xi,\mathfrak{S}_n(\xi))-K_1(\xi,\mathfrak{S}_{n-1}(\xi))\|\\ &\quad+\frac{\beta_1}{B(\beta_1)\Gamma(\beta_1)}\int_0^{\xi}(\xi-s)^{\beta_1-1}\|k_1(s,\mathfrak{S}_n(s))-k_1(s,\mathfrak{S}_{n-1}(s))\|ds,\end{aligned} \tag{4.27}$$

$$\begin{aligned}\|\ G\mathfrak{I}_{H_{n+1}}(\xi)\| &= \|\mathfrak{I}_{H_{n+1}}-\mathfrak{I}_{H_n}\|(\xi)\\ &= \frac{1-\beta_2}{B(\beta_2)}\left\|K_2(\xi,\mathfrak{I}_{H_n}(\xi))-K_2(\xi,\mathfrak{I}_{H_{n-1}}(\xi))\right\|\\ &\quad+\frac{\beta_2}{B(\beta_2)\Gamma(\beta_2)}\int_0^{\xi}(\xi-s)^{\beta_1-1}\|k_2(s,\mathfrak{I}_{H_n}(s))-k_2(s,\mathfrak{I}_{H_{n-1}}(s))\|ds,\end{aligned} \tag{4.28}$$

$$\begin{aligned}\|G\mathfrak{I}_{NE_{n+1}}(\xi)\| &= \|\mathfrak{I}_{NE_{n+1}}-\mathfrak{I}_{NE_n}\|(\xi)\\ &= \frac{1-\beta_3}{B(\beta_3)}\left\|K_3(\xi,\mathfrak{I}_{NE_n}(\xi))-K_3(\xi,\mathfrak{I}_{NE_{n-1}}(\xi))\right\|\\ &\quad+\frac{\beta_3}{B(\beta_3)\Gamma(\beta_3)}\int_0^{\xi}(\xi-s)^{\beta_3-1}\|K_3(s,\mathfrak{I}_{NE_n}(s))-k_3(s,\mathfrak{I}_{NE_{n-1}}(s))\|ds,\end{aligned} \tag{4.29}$$

$$\begin{aligned}\|G\mathfrak{I}_{N_{n+1}}(\xi)\| &= \|\mathfrak{I}_{N_{n+1}}-\mathfrak{I}_{N_n}\|(\xi)\\ &= \frac{1-\beta_4}{B(\beta_4)}\left\|K_4(\xi,\mathfrak{I}_{N_n}(\xi))-K_4(\xi,\mathfrak{I}_{H_{n-1}}(\xi))\right\|\\ &\quad+\frac{\beta_4}{B(\beta_4)\Gamma(\beta_4)}\int_0^{\xi}(\xi-s)^{\beta_4-1}\|K_4(s,\mathfrak{I}_{N_n}(s))-k_4(s,\mathfrak{I}_{N_{n-1}}(s))\|ds,\end{aligned} \tag{4.30}$$

$$\begin{aligned}\|G\mathfrak{R}_{n+1}(\xi)\| &= \|\mathfrak{R}_{n+1}-\mathfrak{R}_n\|(\xi)\\ &= \frac{1-\beta_5}{B(\beta_5)}\|K_5(\xi,\mathfrak{R}_n(\xi))-K_5(\xi,\mathfrak{R}_{n-1}(\xi))\|\\ &\quad+\frac{\beta_5}{B(\beta_5)\Gamma(\beta_5)}\int_0^{\xi}(\xi-s)^{\beta_5-1}\|k_5(s,\mathfrak{R}_n(s))-k_5(s,\mathfrak{R}_{n-1}(s))\|ds.\end{aligned} \tag{4.31}$$

Theorem 4.2. *There is a solution for the fractional order EBOV-NIV co-infection treatment model* (3.1)*, given that the following constraint is met*

$$\Delta = max\{\phi_i\} < 1, \ \textit{where } i \in N_1^5. \tag{4.32}$$

Proof. Define the functions

$$\nu 1_n(\xi) = \mathfrak{S}_{n-1}(\xi) - \mathfrak{S}(\xi), \tag{4.33}$$

$$\nu 2_n(\xi) = \mathfrak{I}_{H_{n-1}}(\xi) - \mathfrak{I}_H(\xi), \tag{4.34}$$

$$\nu 3_n(\xi) = \mathfrak{I}_{NE_{n-1}}(\xi) - \mathfrak{I}_{NE}(\xi), \tag{4.35}$$

$$\nu 4_n(\xi) = \mathfrak{I}_{N_{n-1}}(\xi) - \mathfrak{I}_N(\xi), \tag{4.36}$$

$$\nu 5_n(\xi) = \mathfrak{R}_{n-1}(\xi) - \mathfrak{R}(\xi). \tag{4.37}$$

By using the equation (2.1) to (4.37) we find,

$$\begin{aligned}\|\nu 1_n(\xi)\| &\leq \frac{1-\beta_1}{B(\beta_1)}\|K_1(\xi,\mathfrak{S}_n(\xi)) - K_1(\xi,\mathfrak{S}(\xi))\| \\ &\quad + \frac{\beta_1}{B(\beta_1)\Gamma(\beta)}\int_0^\xi (\xi-s)^{\beta_1-1}\|K_1(S,\mathfrak{S}_n(s)) - K_1(S,\mathfrak{S}(s))\|ds \\ &\leq \left[\frac{1-\beta_1}{B(\beta_1)} + \frac{\beta_1}{B(\beta_1)\Gamma(\beta)}\right]\Delta^n\|\mathfrak{S}-\mathfrak{S}_1\|. \end{aligned} \tag{4.38}$$

Next,

$$\begin{aligned}\|\nu 2_n(\xi)\| &\leq \frac{1-\beta_2}{B(\beta_2)}\|K_2(\xi,\mathfrak{I}_{H_n}(\xi)) - K_2(\xi,\mathfrak{I}_H(\xi))\| \\ &\quad + \frac{\beta_2}{B(\beta_2)\Gamma(\beta_2)}\int_0^\xi (\xi-s)^{\beta_2-1}\|K_2(S,\mathfrak{I}_{H_n}(s)) - K_2(S,\mathfrak{I}_H(s))\|ds \\ &\leq \left[\frac{1-\beta_2}{B(\beta_2)} + \frac{\beta_2}{B(\beta_2)\Gamma(\beta_2)}\right]\phi_2\|\mathfrak{I}_{H_n} - \mathfrak{I}_H\| \\ &\leq \Delta^n\|\mathfrak{I}_H - \mathfrak{I}_{H_1}\|. \end{aligned} \tag{4.39}$$

And also,

$$\begin{aligned}\|\nu 3_n(\xi)\| &\leq \frac{1-\beta_3}{B(\beta_3)}\|K_3(\xi,\mathfrak{I}_{NE_n}(\xi)) - K_3(\xi,\mathfrak{I}_{NE}(\xi))\| \\ &\quad + \frac{\beta_3}{B(\beta_3)\Gamma(\beta_3)}\int_0^\xi (\xi-s)^{\beta_3-1}\|K_3(S,\mathfrak{I}_{NE_n}(s)) - K_3(S,\mathfrak{I}_{NE}(s))\|ds \\ &\leq \left[\frac{1-\beta_3}{B(\beta_3)} + \frac{\beta_3}{B(\beta_3)\Gamma(\beta_3)}\right]\phi_3\|\mathfrak{I}_{NE_n} - \mathfrak{I}_{NE}\| \\ &\leq \left[\frac{1-\beta_3}{B(\beta_3)} + \frac{\beta_3}{B(\beta_3)\Gamma(\beta_3)}\right]\Delta^n\|\mathfrak{I}_{NE} - \mathfrak{I}_{NE_1}\|. \end{aligned} \tag{4.40}$$

From the above equations, we find $\nu_i(\xi)_n \to 0$ as $n \to \infty$, $i \in N^5$ for $\Delta, 1$. This completes the proof. □

The following theorem is for the uniqueness of solution.

Theorem 4.3. *If the constraints mentioned in Equation* (4.41) *are satisfied, then AB fractional order model* 2.1 *possesses a singular solution, when the following conditions are hold*

$$\left[\frac{1-\beta_i}{B(\beta_i)}+\frac{\beta_i}{B(\beta_i)\Gamma(\beta_i)}\right]\phi_i \leq 1, \quad i \in N_1^5. \tag{4.41}$$

Proof. Let $(\widetilde{\mathfrak{S}}(\xi), \widetilde{\mathfrak{I}_E}(\xi), \widetilde{\mathfrak{I}_{NE}}(\xi), \widetilde{\mathfrak{I}_N}(\xi), \widetilde{\mathfrak{I}_R}(\xi))$ be a another solution for the system. Then we have

$$\widetilde{\mathfrak{S}}(\xi) = \frac{1-\beta_1}{B(\beta_1)}K_1(\xi, \widetilde{\mathfrak{S}}(\xi)) + \frac{\beta_1}{B(\beta_1)\Gamma(\beta_1)}\int_0^\xi (\xi-s)^{\beta_1-1}K_1(\mathfrak{S}, \widetilde{\mathfrak{S}}(s))ds, \tag{4.42}$$

$$\widetilde{\mathfrak{I}_E}(\xi) = \frac{1-\beta_2}{B(\beta_2)}K_2(\xi, \widetilde{\mathfrak{I}_E}(\xi)) + \frac{\beta_2}{B(\beta_2)\Gamma(\beta_2)}\int_0^\xi (\xi-s)^{\beta_2-1}K_2(\mathfrak{S}, \widetilde{\mathfrak{I}_E}(s))ds, \tag{4.43}$$

$$\widetilde{\mathfrak{I}_{NE}}(\xi) = \frac{1-\beta_3}{B(\beta_3)}K_3(\xi, \widetilde{\mathfrak{I}_{NE}}(\xi)) + \frac{\beta_3}{B(\beta_3)\Gamma(\beta_3)}\int_0^\xi (\xi-s)^{\beta_3-1}K_3(\mathfrak{S}, \widetilde{\mathfrak{I}_{NE}}(s))ds, \tag{4.44}$$

$$\widetilde{\mathfrak{I}_N}(\xi) = \frac{1-\beta_4}{B(\beta_4)}K_4(\xi, \widetilde{\mathfrak{I}_N}(\xi)) + \frac{\beta_4}{B(\beta_4)\Gamma(\beta_4)}\int_0^\xi (\xi-s)^{\beta_4-1}K_4(\mathfrak{S}, \widetilde{\mathfrak{I}_N}(s))ds, \tag{4.45}$$

$$\widetilde{\mathfrak{I}_R}(\xi) = \frac{1-\beta_5}{B(\beta_5)}K_5(\xi, \widetilde{\mathfrak{I}_R}(\xi)) + \frac{\beta_5}{B(\beta_5)\Gamma(\beta_5)}\int_0^\xi (\xi-s)^{\beta_5-1}K_5(\mathfrak{S}, \widetilde{\mathfrak{I}_R}(s))ds. \tag{4.46}$$

By using equations (4.42) to (4.46) and Theorem 4.2, we take the norm,

$$\begin{aligned}\|\mathfrak{S}(\xi) - \widetilde{\mathfrak{S}}(\xi)\| &\leq \frac{1-\beta_1}{B(\beta_1)}\|K_1(\xi, \mathfrak{S}(\xi)) - K_1(\xi, \widetilde{\mathfrak{S}}(\xi))\| \\ &\quad + \frac{\beta_1}{B(\beta_1)\Gamma(\beta_1)}\int_0^\xi (\xi-s)^{\beta_1-1}\|K_1(s, \mathfrak{S}(s)) - K_1(s, \widetilde{\mathfrak{S}}(s))\| \\ &\leq \frac{1-\beta_1}{B(\beta_1)}\phi_1\|\mathfrak{S} - \widetilde{\mathfrak{S}}\| + \frac{\phi_1}{B(\beta_1)\Gamma(\beta_1)}\|\mathfrak{S} - \widetilde{\mathfrak{S}}\|.\end{aligned}$$

This implies that

$$\left[\frac{1-\beta_1}{B(\beta_1)}\phi_1 + \frac{\phi_1}{B(\beta_1)\Gamma(\beta_1)}\right]\|\mathfrak{S} - \widetilde{\mathfrak{S}}\| \geq 0. \tag{4.47}$$

By condition (4.43), the inequality (4.47) is true, than we have

$$\|\mathfrak{S} - \widetilde{\mathfrak{S}}\| = 0,$$

that is,

$$\mathfrak{S}(\xi) = \widetilde{\mathfrak{S}}(\xi). \tag{4.48}$$

Likewise, we demonstrate that, using the same method,

$$\begin{aligned}\mathfrak{I}_E(\xi) &= \widetilde{\mathfrak{I}_E}(\xi),\\ \mathfrak{I}_{NE}(\xi) &= \widetilde{\mathfrak{I}_{NE}}(\xi),\\ \mathfrak{I}_N(\xi) &= \widetilde{\mathfrak{I}_N}(\xi),\\ \mathfrak{I}_R(\xi) &= \widetilde{\mathfrak{I}_R}(\xi).\end{aligned} \tag{4.49}$$

Thus, there is just one solution for the model (2.1). □

5. Hyers-Ulam stability

In this section the authors discussed the H-U stability of ABC fractional integral system in the described by equations (4.17) to (4.21).

Definition 5.1. The AB fractional integral system described by equations (4.17) to (4.21) is considered H-U stable if exist constants $\Delta_i > 0$, $i \in N_1^5$ such that for every $\gamma_i > 0$, $i \in N_1^5$ for which

$$\left|\mathfrak{S}(\xi) - \frac{1-\beta_1}{B(\beta_1)}K_1(\xi,\mathfrak{S}(\xi)) + \frac{\beta_1}{B(\beta_1)\Gamma(\beta_1)}\int_0^\xi (\xi-s)^{\beta_1-1}K_1(s,\mathfrak{S}(s))ds\right| \le \gamma_1, \tag{5.1}$$

$$\left|\mathfrak{I}_E(\xi) - \frac{1-\beta_2}{B(\beta_2)}K_2(\xi,\mathfrak{I}_E(\xi)) + \frac{\beta_2}{B(\beta_2)\Gamma(\beta_2)}\int_0^\xi (\xi-s)^{\beta_2-1}K_2(s,\mathfrak{I}_E(s))ds\right| \le \gamma_2, \tag{5.2}$$

$$\left|\mathfrak{I}_{NE}(\xi) - \frac{1-\beta_3}{B(\beta_3)}K_3(\xi,\mathfrak{I}_{NE}(\xi)) + \frac{\beta_3}{B(\beta_3)\Gamma(\beta_3)}\int_0^\xi (\xi-s)^{\beta_3-1}K_3(s,\mathfrak{I}_{NE}(s))ds\right| \le \gamma_3, \tag{5.3}$$

$$\left|\mathfrak{I}_N(\xi) - \frac{1-\beta_4}{B(\beta_4)}K_4(\xi,\mathfrak{I}_N(\xi)) + \frac{\beta_4}{B(\beta_4)\Gamma(\beta_4)}\int_0^\xi (\xi-s)^{\beta_4-1}K_4(s,\mathfrak{I}_N(s))ds\right| \le \gamma_4, \tag{5.4}$$

$$\left|\mathfrak{R}(\xi) - \frac{1-\beta_5}{B(\beta_5)}K_5(\xi,\mathfrak{R}(\xi)) + \frac{\beta_5}{B(\beta_5)\Gamma(\beta_5)}\int_0^\xi (\xi-s)^{\beta_5-1}K_5(s,\mathfrak{R}(s))ds\right| \le \gamma_5, \tag{5.5}$$

there exist ($\dot{\mathfrak{S}}$, $\dot{\mathfrak{I}_E}$, $\dot{\mathfrak{I}_{NE}}$, $\dot{\mathfrak{I}_N}$, $\dot{\mathfrak{R}}$) which are satisfying

$$\dot{\mathfrak{S}}(\xi) = \frac{1-\beta_1}{B(\beta_1)}K_1(\xi,\dot{\mathfrak{S}}(\xi)) + \frac{\beta_1}{B(\beta_1)\Gamma(\beta_1)}\int_0^\xi (\xi-s)^{\beta_1-1}K_1(s,\dot{\mathfrak{S}}(s))ds, \tag{5.6}$$

$$\dot{\mathfrak{I}_E}(\xi) = \frac{1-\beta_2}{B(\beta_2)} K_2(\xi, \dot{\mathfrak{I}_E}(\xi)) + \frac{\beta_2}{B(\beta_2)\Gamma(\beta_2)} \int_0^\xi (\xi - s)^{\beta_2 - 1} K_2(s, \dot{\mathfrak{I}_E}(s)) ds, \quad (5.7)$$

$$\dot{\mathfrak{I}_{NE}}(\xi) = \frac{1-\beta_3}{B(\beta_3)} K_3(\xi, \dot{\mathfrak{I}_{NE}}(\xi)) + \frac{\beta_3}{B(\beta_3)\Gamma(\beta_3)} \int_0^\xi (\xi - s)^{\beta_3 - 1} K_3(s, \dot{\mathfrak{I}_{NE}}(s)) ds, \quad (5.8)$$

$$\dot{\mathfrak{I}_N}(\xi) = \frac{1-\beta_4}{B(\beta_4)} K_4(\xi, \dot{\mathfrak{I}_N}(\xi)) + \frac{\beta_4}{B(\beta_4)\Gamma(\beta_4)} \int_0^\xi (\xi - s)^{\beta_4 - 1} K_4(s, \dot{\mathfrak{I}_N}(s)) ds, \quad (5.9)$$

$$\dot{\mathfrak{R}}(\xi) = \frac{1-\beta_5}{B(\beta_5)} K_5(\xi, \dot{\mathfrak{R}}(\xi)) + \frac{\beta_5}{B(\beta_5)\Gamma(\beta_5)} \int_0^\xi (\xi - s)^{\beta_5 - 1} K_5(s, \dot{\mathfrak{R}}(s)) ds, \quad (5.10)$$

such that

$$\begin{aligned} |\mathfrak{S}(\xi) - \dot{\mathfrak{S}}(\xi)| &\leq \lambda_1 \gamma_1, \\ |\mathfrak{I}_E(\xi) - \dot{\mathfrak{I}_E}(\xi)| &\leq \lambda_2 \gamma_2, \\ |\mathfrak{I}_{NE}(\xi) - \dot{\mathfrak{I}_{NE}}(\xi)| &\leq \lambda_3 \gamma_3, \\ |\mathfrak{I}_N(\xi) - \dot{\mathfrak{I}_N}(\xi)| &\leq \lambda_4 \gamma_4, \\ |\mathfrak{R}(\xi) - \dot{\mathfrak{R}}(\xi)| &\leq \lambda_5 \gamma_5. \end{aligned} \quad (5.11)$$

Theorem 5.2. *Given B, the suggested fractional order model* (3.1) *is H-U stable.*

Proof. The unique solution to the suggested AB fractional model (3.1), may be found using Theorem 4.3, ($\mathfrak{S}(\xi)$, $\mathfrak{I}_E(\xi)$, $\mathfrak{I}_{NE}(\xi)$, $\mathfrak{I}_N(\xi)$, $\mathfrak{R}(\xi)$).

Suppose $(\dot{\mathfrak{S}}, \dot{\mathfrak{I}_E}, \dot{\mathfrak{I}_{NE}}, \dot{\mathfrak{I}_N}, \dot{\mathfrak{R}})$ is an approximate solution to model 3 that satisfies equations (4.17) to (4.21). Then, we have

$$\begin{aligned} \|\mathfrak{S}(\xi) - \dot{\mathfrak{S}}(\xi)\| &\leq \frac{1-\beta_1}{B(\beta_1)} \|K_1(\xi, \mathfrak{S}(\xi)) - K_1(\xi, \dot{\mathfrak{S}}(\xi))\| \\ &\quad + \frac{\beta_1}{B(\beta_1)\Gamma(\beta_1)} \int_0^\xi (\xi - s)^{\beta_1 - 1} \|K_1(s, \mathfrak{S}(s)) - K_1(s, \dot{\mathfrak{S}}(s))\| ds \\ &\leq \left[\frac{1-\beta_1}{B(\beta_1)} + \frac{1}{B(\beta_1)\Gamma(\beta_1)} \right] \phi_1 \|\mathfrak{S} - \dot{\mathfrak{S}}\|. \end{aligned}$$

Let $\gamma_1 = \phi_1$ and $\Delta_1 = \frac{1-\beta_1}{B(\beta_1)} + \frac{1}{B(\beta_1)\Gamma(\beta_1)}$, we get

$$\|\mathfrak{S}(\xi) - \dot{\mathfrak{S}}(\xi)\| \leq \gamma_1 \Delta_1. \quad (5.12)$$

Similarly, we get

$$\|\mathfrak{I}_E(\xi) - \dot{\mathfrak{I}_E}(\xi)\| \leq \gamma_2 \Delta_2, \quad (5.13)$$

$$\|\mathfrak{I}_{NE}(\xi) - \dot{\mathfrak{I}_{NE}}(\xi)\| \leq \gamma_3 \Delta_3, \tag{5.14}$$

$$\|\mathfrak{I}_{N}(\xi) - \dot{\mathfrak{I}_{N}}(\xi)\| \leq \gamma_4 \Delta_4, \tag{5.15}$$

$$\|\mathfrak{R}(\xi) - \dot{\mathfrak{R}}(\xi)\| \leq \gamma_5 \Delta_5. \tag{5.16}$$

Utilizing equations (5.12) and (5.16), we establish the H-U stability of the AB fractional integral system (4.17) to (4.21), and consequently, the H-U stability of the AB-fractional order model (3.1). This concludes the proof. □

6. Numerical simulation

Finding the exact solution of fractional differential equations is very difficult. Therefore, most of the researchers investigating fractional differential equations optimize and approximate the solution by applying pre-existing techniques. For the numerical solution, they applied modified Euler techniques, Taylor's series method, Adams-Bash-Forth techniques, the predictor-corrector method, and different integral transforms.

The methodology in this work integrates fractal geometry and scaling concepts with fractional-order calculus to model the dynamics of Ebola and Nipah virus co-infection. We investigate the stability and qualitative characteristics of the system using Hyers-Ulam stability theory and fixed-point theory. The theoretical framework is supplemented with numerical simulations that provide a detailed analysis of the behavior of the viruses using the fractional Atangana-Baleanu integral and the Adams-Milton methods in Matlab. We also verify our model and clarify the complex dynamics and patterns resulting from co-infections. This thorough method offers insightful information about intricate relationships and scaling patterns in the dynamics of viral transmission.

We now show the numerical simulation of model with various non-integer order derivatives 6.2 we study the dynamical behaviour of the model of variation of the non-integer order derivative β_i, $i = 1, 2, 3, 4, 5$. In order to evaluate the approximate answer, $h = 0.001$ was the step-size employed.

Alkahtani [14] provides the computational estimation of the Atangana-Baleanu fractional integral utilizing the Adams-Moulton rule.

$${}_0^{AB}L_i^{\beta}[\phi(\xi_{n+1})] = \frac{1-\beta}{B(\beta)}\left[\frac{\phi(\xi_{n+1})-\phi(\xi_n)}{2}\right] + \frac{\beta}{B(\beta)\Gamma(\beta)}\sum_{k=0}^{\infty}\left[\frac{\phi(\xi_{k+1})-\phi(\xi_k)}{2}\right] b_k^{\beta}, \tag{6.1}$$

where $b_k^{\beta} = (k+1)^{1-\beta} - (k)^{1-\beta}$.

Employing the numerical scheme described above, we obtain:

$$
\begin{aligned}
&\mathfrak{S}_{n+1}(\xi)-\mathfrak{S}_n(\xi)\\
&\quad=\mathfrak{S}_0^n(\xi)+\left\{\frac{1-\beta_1}{B(\beta_1)}\left[\wedge-\frac{\beta_E}{N}\left(\frac{\mathfrak{I}_{E_{n+1}}(\xi)-\mathfrak{I}_{E_n}(\xi)}{2}\right)+\left(\frac{\mathfrak{I}_{EN}(\xi)-\mathfrak{I}_{EN_n}(\xi)}{2}\right)\right.\right.\\
&\qquad\left.\left.+\frac{\beta_E}{N}\left(\frac{\mathfrak{I}_{N_{n+1}}(\xi)-\mathfrak{I}_{N_n}(\xi)}{2}\right)+\left(\frac{\mathfrak{S}(\xi)-\mathfrak{S}_n(\xi)}{2}\right)\right]\right\}\\
&\qquad+\frac{\beta_1}{B(\beta_1)}\sum_{k=0}^{\infty}b_k^{\beta_1}\left[\wedge-\frac{\beta_E}{N}\left(\frac{\mathfrak{I}_{E_{k+1}}(\xi)-\mathfrak{I}_{E_k}(\xi)}{2}\right)+\left(\frac{\mathfrak{I}_{EN_{k+1}}(\xi)-\mathfrak{I}_{EN_k}(\xi)}{2}\right)\right.\\
&\qquad\left.+\frac{\beta_N}{N}\left(\frac{\mathfrak{I}_{N_{k+1}}(\xi)-\mathfrak{I}_{N_k}(\xi)}{2}\right)+\left(\frac{\mathfrak{I}_{NE_{k+1}}(\xi)-\mathfrak{I}_{NE_k}(\xi)}{2}\right)+\mu\left(\frac{\mathfrak{S}_{k+1}(\xi)-\mathfrak{S}_k(\xi)}{2}\right)\right],
\end{aligned}
$$

$$
\begin{aligned}
&\mathfrak{I}_{E_{n+1}}(\xi)-\mathfrak{I}_{E_n}(\xi)\\
&\quad=\mathfrak{I}_{E_0}^n(\xi)+\left\{\frac{1-\beta_2}{B(\beta_2)}\left[\frac{\beta_E}{N}\left(\frac{\mathfrak{I}_{E_{n+1}}(\xi)-\mathfrak{I}_{E_n}(\xi)}{2}\right)+\left(\frac{\mathfrak{I}_{NE}(\xi)-\mathfrak{I}_{NE_n}(\xi)}{2}\right)\right.\right.\\
&\qquad+\left(\frac{\mathfrak{S}_{(n+1)}(\xi)-\mathfrak{S}_n(\xi)}{2}\right)-(\mu+\delta_1+\omega_1)\left(\frac{\mathfrak{I}_{E_{n+1}}-\mathfrak{I}_{E_n}(\xi)}{2}\right)\\
&\qquad\left.\left.+\ \eta_1\left(\frac{\mathfrak{I}_{N_{n+1}}-\mathfrak{I}_{N_n}(\xi)}{2}\right)\left(\frac{\mathfrak{I}_{NE_{n+1}}-\mathfrak{I}_{NE_n}(\xi)}{2}\right)\left(\frac{\mathfrak{I}_{E_{n+1}}-\mathfrak{I}_{E_n}(\xi)}{2}\right)\right]\right\}\\
&\qquad+\frac{\beta_1}{B(\beta_1)}\sum_{k=0}^{\infty}b_k^{\beta_1}\left[\frac{\beta_E}{N}\left(\frac{\mathfrak{I}_{E_{n+1}}(\xi)-\mathfrak{I}_{E_n}(\xi)}{2}\right)+\left(\frac{\mathfrak{I}_{NE}(\xi)-\mathfrak{I}_{NE_n}(\xi)}{2}\right)\right.\\
&\qquad+\left(\frac{\mathfrak{S}_{(n+1)}(\xi)-\mathfrak{S}_n(\xi)}{2}\right)-(\mu+\delta_1+\omega_1)\left(\frac{\mathfrak{I}_{E_{n+1}}-\mathfrak{I}_{E_n}(\xi)}{2}\right)\\
&\qquad\left.+\eta_1\left(\frac{\mathfrak{I}_{N_{n+1}}-\mathfrak{I}_{N_n}(\xi)}{2}\right)\left(\frac{\mathfrak{I}_{NE_{n+1}}-\mathfrak{I}_{NE_n}(\xi)}{2}\right)\left(\frac{\mathfrak{I}_{E_{n+1}}-\mathfrak{I}_{E_n}(\xi)}{2}\right)\right],
\end{aligned}
$$

$$
\begin{aligned}
&\mathfrak{I}_{NE_{n+1}}(\xi)-\mathfrak{I}_{NE_n}(\xi)\\
&\quad=\mathfrak{I}_{NE_0}^n(\xi)+\left\{\frac{1-\beta_3}{B(\beta_3)}\left[\eta_1\frac{\beta_N}{N}\left(\frac{\mathfrak{I}_{N_{n+1}}(\xi)-\mathfrak{I}_{N_n}(\xi)}{2}\right)+\left(\frac{\mathfrak{I}_{NE}(\xi)-\mathfrak{I}_{NE_n}(\xi)}{2}\right)\right.\right.\\
&\qquad+\left(\frac{\mathfrak{I}_{\mathfrak{E}_{n+1}}(\xi)-\mathfrak{I}_{E_n}(\xi)}{2}\right)+\eta_2\frac{\beta_E}{N}\left(\frac{\mathfrak{I}_{E_{n+1}}(\xi)-\mathfrak{I}_{E_n}(\xi)}{2}\right)\\
&\qquad+\left(\frac{\mathfrak{I}_{NE}(\xi)-\mathfrak{I}_{NE_n}(\xi)}{2}\right)\left(\frac{\mathfrak{I}_{N_{n+1}}(\xi)-\mathfrak{I}_{N_n}(\xi)}{2}\right)\\
&\qquad\left.\left.-(\mu+\delta_3+\omega_2)\left(\frac{\mathfrak{I}_{NE_{n+1}}-\mathfrak{I}_{NE_n}(\xi)}{2}\right)\right]\right\}
\end{aligned}
$$

$$
\begin{aligned}
&+\frac{\beta_3}{B(\beta_3)}\sum_{k=0}^{\infty} b_k^{\beta_3}\left[\eta_2\frac{\beta_E}{N}\left(\frac{\mathfrak{I}_{E_{k+1}}(\xi)-\mathfrak{I}_{E_k}(\xi)}{2}\right)\right.\\
&+\left(\frac{\mathfrak{I}_{NE_{k+1}}(\xi)-\mathfrak{I}_{NE_k}(\xi)}{2}\right)+\left(\frac{\mathfrak{I}_{N_{k+1}}(\xi)-\mathfrak{I}_{N_k}(\xi)}{2}\right)\\
&\left.-(\mu+\delta_3+\omega_2)\left(\frac{\mathfrak{I}_{NE_{k+1}}(\xi)-\mathfrak{I}_{NE_k}(\xi)}{2}\right)\right],
\end{aligned}
$$

$$
\begin{aligned}
&\mathfrak{I}_{N_{n+1}}(\xi)-\mathfrak{I}_{N_n}(\xi)\\
&=\mathfrak{I}^n_{N_0}(\xi)+\left\{\frac{1-\beta_4}{B(\beta_4)}\left[\frac{\beta_N}{N}\left(\frac{\mathfrak{I}_{N_{n+1}}(\xi)-\mathfrak{I}_{N_n}(\xi)}{2}\right)+\left(\frac{\mathfrak{I}_{NE}(\xi)-\mathfrak{I}_{NE_n}(\xi)}{2}\right)\right.\right.\\
&+\left(\frac{\mathfrak{S}_{n+1}(\xi)-\mathfrak{S}_n(\xi)}{2}\right)-(\mu+\delta_2+\eta_2)\left(\frac{\mathfrak{I}_{E_{n+1}}(\xi)-\mathfrak{I}_{E_n}(\xi)}{2}\right)\frac{\beta_E}{N}\\
&\left.\left.-(\mu+\delta_2+\eta_2)\left(\frac{\mathfrak{I}_{NE}(\xi)-\mathfrak{I}_{NE_n}(\xi)}{2}\right)\frac{\beta_E}{N}+\omega_3\right]\right\}\\
&\times\left(\frac{\mathfrak{I}_{N_{n+1}}(\xi)-\mathfrak{I}_{N_n}(\xi)}{2}\right)\\
&+\frac{\beta_4}{B(\beta_4)}\sum_{k=0}^{\infty} b_k^{\beta_4}\left[\frac{\beta_N}{N}\left(\left(\frac{\mathfrak{I}_{N_{k+1}}(\xi)-\mathfrak{I}_{N_k}(\xi)}{2}\right)+\left(\frac{\mathfrak{I}_{NE_{k+1}}(\xi)-\mathfrak{I}_{NE_k}(\xi)}{2}\right)\right)\right.\\
&+\left(\frac{\mathfrak{S}_{k+1}(\xi)-\mathfrak{S}_k(\xi)}{2}\right)-\left\{\left(\mu+\delta_2+\eta_2\frac{\beta_E}{N}\left(\frac{\mathfrak{I}_{NE_{k+1}}(\xi)-\mathfrak{I}_{NE_k}(\xi)}{2}\right)\right)\right.\\
&\left.\left.+\left(\left(\mu+\delta_2+\eta_2\frac{\beta_E}{N}\left(\frac{\mathfrak{I}_{NE_{k+1}}(\xi)-\mathfrak{I}_{NE_k}(\xi)}{2}\right)\right)+\omega_3\right)\right\}\right.\\
&\left.\times\left(\frac{\mathfrak{I}_{N_{k+1}}(\xi)-\mathfrak{I}_{N_k}(\xi)}{2}\right)\right],
\end{aligned}
$$

$$
\begin{aligned}
&\mathfrak{R}_{n+1}(\xi)-\mathfrak{R}_n(\xi)\\
&=\mathfrak{R}^n_0(\xi)+\left\{\frac{1-\beta_5}{B(\beta_5)}\left[\omega_1\left(\frac{\mathfrak{I}_{E_{n+1}}(\xi)-\mathfrak{I}_{E_n}(\xi)}{2}\right)+\omega_2\left(\frac{\mathfrak{I}_{NE_{n+1}}(\xi)-\mathfrak{I}_{NE_n}(\xi)}{2}\right)\right.\right.\\
&\left.\left.+\omega_3\left(\frac{\mathfrak{I}_{N_{n+1}}(\xi)-\mathfrak{I}_{N_n}(\xi)}{2}\right)-\mu\left(\frac{\mathfrak{R}_{n+1}(\xi)-\mathfrak{R}_n(\xi)}{2}\right)\right]\right\}\\
&+\frac{\beta_5}{B(\beta_5)}\sum_{k=0}^{\infty} b_k^{\beta_5}\left[\omega_1\left(\frac{\mathfrak{I}_{E_{k+1}}(\xi)-\mathfrak{I}_{E_k}(\xi)}{2}\right)\right.\\
&+\omega_2\left(\frac{\mathfrak{I}_{NE_{k+1}}(\xi)-\mathfrak{I}_{NE_k}(\xi)}{2}\right)+\omega_3\left(\frac{\mathfrak{I}_{N_{k+1}}(\xi)-\mathfrak{I}_{N_k}(\xi)}{2}\right)\\
&\left.-\mu\left(\frac{\mathfrak{R}_{k+1}(\xi)-\mathfrak{R}_k(\xi)}{2}\right)\right].
\end{aligned}
\tag{6.2}
$$

Parameters	Description
$\wedge$	Rate of population recruitment
λ_E	Rate at which Ebola is transmitted
λ_N	Rate at which Nipah is transmitted
δ_1	Mortality rate associated with Ebola
δ_2	Mortality rate associated with Nipah
δ_3	Mortality rate due to co-infection from both viruses
ω_1	Rate of recovery from Ebola
ω_2	Rate of recovery from Nipah
ω_3	Rate of recovery from both infections
η_1	Level of latency for Ebola-infected individuals becoming asymptotically infected with Nipah
η_2	Rate of susceptibility of Nipah-infected individuals to Ebola
μ	Natural mortality rate

This document provides a detailed analysis of the given image, which consists of five line plots illustrating the population dynamics related to the spread of Ebola and Nipah virus infections over a 10-day period. The analysis focuses on different compartments of the population, including susceptible individuals, infected individuals (both Ebola and Nipah), co-infected individuals, and recovered individuals.

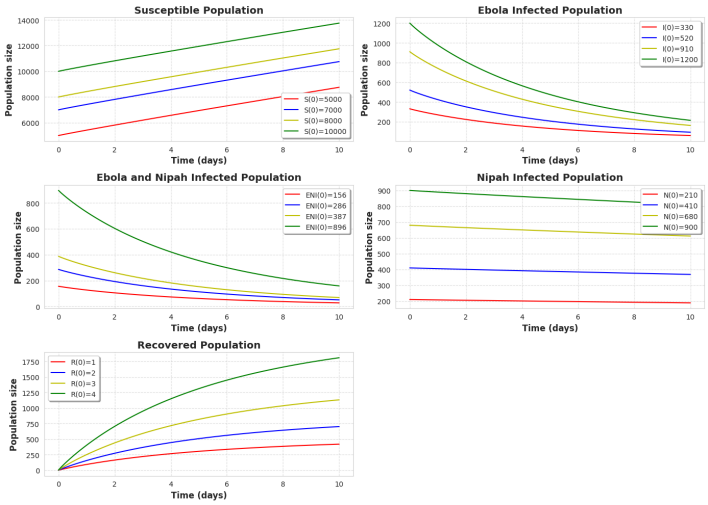

FIGURE 2. Population dynamics of susceptible, infected, co-infected, and recovered individuals over time. Each graph represents different initial conditions.

The figure consists of five subplots:

Susceptible Population

- This subplot (top-left) shows the number of susceptible individuals decreasing over time.
- Different initial conditions ($S(0) = 5000, 7000, 8000, 10000$) are represented in red, blue, yellow, and green curves, respectively.
- Higher initial population sizes correspond to a slower decline, highlighting the impact of initial conditions on disease spread.

Ebola Infected Population

- The top-right subplot illustrates the decline in the Ebola-infected population over time.
- The initial conditions ($I(0) = 330, 520, 910, 1200$) correspond to different curves.
- The decline is more rapid in cases with higher initial infection numbers, suggesting faster recovery or mortality.

Ebola and Nipah Co-Infected Population

- The middle-left subplot represents the number of co-infected individuals.
- The trends show a decreasing pattern similar to the Ebola-infected population.
- Higher initial infection levels ($ENI(0) = 156, 286, 387, 896$) lead to a slower decline.

Nipah Infected Population

- The middle-right subplot displays the Nipah-infected population trends.
- Unlike Ebola, the decline is less pronounced, with some curves remaining nearly stable ($N(0) = 210, 410, 680, 900$).
- This indicates a slower progression of Nipah compared to Ebola.

Recovered Population

- The bottom subplot represents the recovered population, which increases over time.
- Different initial conditions ($R(0) = 1, 2, 3, 4$) show varying recovery rates.
- The highest initial recovery (green curve) results in the highest recovered population.

Significance and Interpretation

- The image highlights the progression of disease transmission and recovery dynamics in a fractional-order epidemiological model.
- The faster decline of Ebola-infected and co-infected populations compared to Nipah suggests different disease progression and mortality rates.
- The decrease in the susceptible population aligns with the increase in the recovered population, illustrating the natural resolution of infections.
- Variability in initial conditions significantly affects disease dynamics, reinforcing the importance of early intervention strategies.

This visualization provides insights into disease spread and intervention effectiveness, demonstrating the role of mathematical modeling in epidemiological research.

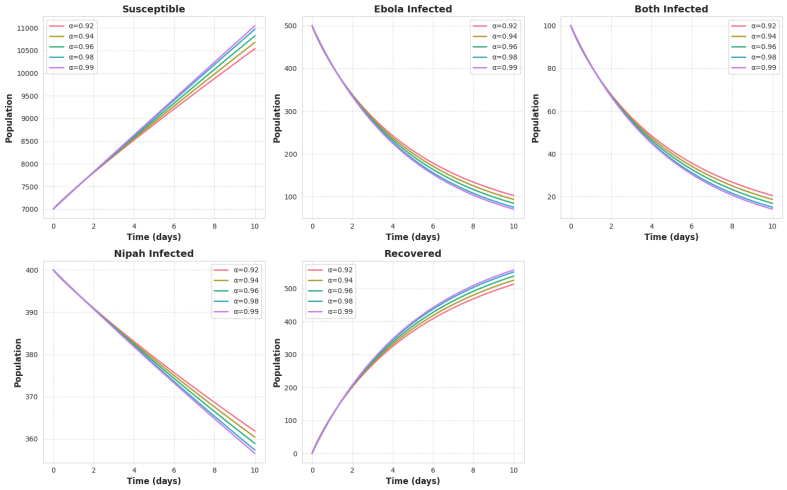

FIGURE 3. Time evolution of different compartments in the epidemic model for varying values of the fractional order parameter α. The subplots depict the susceptible population, Ebola-infected individuals, both Ebola and Nipah co-infected individuals, Nipah-infected individuals, and the recovered population over a period of 10 days. Each curve corresponds to a different α value, as indicated in the legends.

Figure 3 illustrates the temporal dynamics of an epidemic model incorporating fractional calculus. The image comprises five subplots, each representing a distinct compartment of the model: (i) susceptible individuals, (ii) individuals

infected with Ebola, (iii) individuals co-infected with both Ebola and Nipah, (iv) individuals infected with Nipah, and (v) recovered individuals. The x-axis in all subplots represents time (in days), while the y-axis denotes the corresponding population size.

The curves in each subplot correspond to different values of the fractional-order parameter α, ranging from 0.92 to 0.99. As α increases, the model exhibits subtle variations in the population dynamics, highlighting the impact of fractional derivatives on disease progression. Notably, the susceptible population shows an increasing trend, while the infected populations (both Ebola and Nipah) decline over time. The recovered compartment exhibits an upward trend, indicating progressive recovery from infection. These trends align with the expected theoretical behavior of fractional epidemic models.

The visualization provides insights into the sensitivity of the model to variations in α, which is crucial for understanding disease transmission under fractional-order dynamics. The inclusion of multiple α values enables comparative analysis and validation of the model's applicability in real-world epidemiological scenarios.

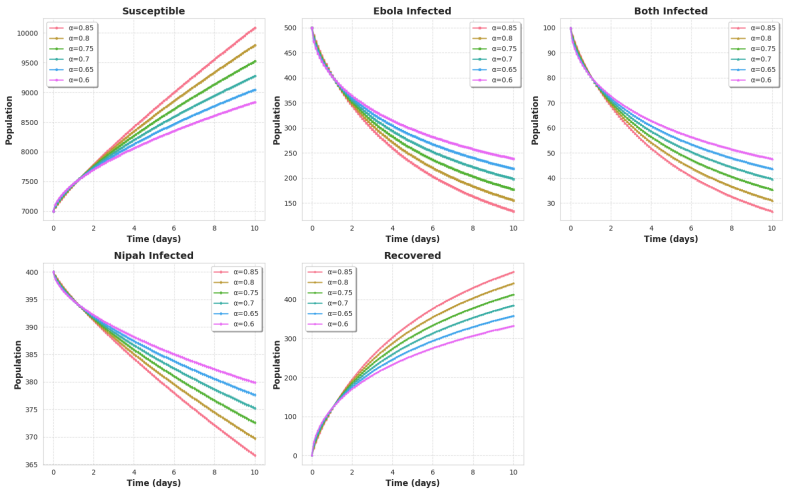

FIGURE 4. Temporal evolution of population compartments in a fractional-order model. Subplots show susceptible, Ebola-infected, co-infected, Nipah-infected, and recovered populations over time for $\alpha \in [0.60, 0.85]$.

The given figure consists of a set of five subplots arranged in a 2×3 grid (with the last slot empty), representing the temporal evolution of different population compartments in a fractional-order epidemiological model. Each

subplot visualizes the population dynamics of specific categories: Susceptible, Ebola Infected, Both Infected (Ebola and Nipah), Nipah Infected, and Recovered individuals. The x-axis in all subplots represents Time (days), while the y-axis represents the corresponding Population size.

Each curve in the plots corresponds to different values of the fractional-order parameter α, ranging from 0.85 to 0.60, as indicated in the legends. The color-coded lines in each graph show how varying α influences the population trajectory. The susceptible population exhibits an increasing trend over time, while the infected categories (Ebola Infected, Nipah Infected, and Both Infected) demonstrate a declining trend. Conversely, the Recovered compartment displays an upward trajectory, indicating disease resolution over time.

The key observations are

(1) **Susceptible Population:** Increases over time due to recruitment. Higher α yields faster growth.
(2) **Ebola and Nipah Infected:** Monotonic decline. Lower α prolongs persistence.
(3) **Both Infected:** Sharp decline at high α, slower clearance at low α.
(4) **Recovered Population:** Steady increase. Faster recovery at higher α.

This figure highlights the influence of the fractional-order parameter α on the disease dynamics. The results indicate that larger α values lead to faster infection clearance and quicker recovery, suggesting a more responsive system. Conversely, lower α values correspond to slower recovery rates, potentially prolonging disease spread. This analysis is crucial for understanding disease control strategies, particularly in designing fractional-order epidemic models to assess intervention efficacy.

The trends and behaviors observed in the plots align with theoretical expectations of fractional-order dynamical systems, where memory effects influence the rate of disease transmission and recovery. These findings contribute to the broader discussion on fractional calculus in epidemiological modeling, emphasizing its applicability in capturing real-world disease dynamics more accurately than traditional integer-order models.

Figure 5 presents a graphical representation of the numerical solution of a fractional-order epidemic model incorporating two infectious diseases, Ebola and Nipah. The plot illustrates the temporal evolution of different population compartments, including Susceptible (S), Infected with Ebola (I_1), Infected with Nipah (I_2), Coinfected Individuals (I_{12}), and Recovered (R), over a period of 10 days.

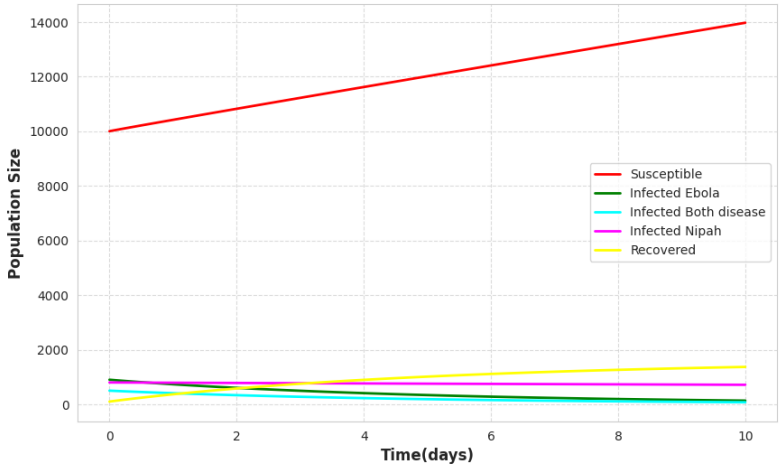

FIGURE 5. Temporal dynamics of population compartments over 10 days in a fractional-order model. Curves: Susceptible (red), Ebola-infected (green), Nipah-infected (magenta), co-infected (cyan), recovered (yellow).

The figure demonstrates the following key trends:

- The susceptible population (red line) exhibits a steady increase over time, indicating continuous recruitment into the population, possibly due to a birth rate term incorporated in the model.
- The Ebola-infected population (green line) initially decreases, reflecting the impact of disease-related mortality and recovery dynamics.
- The Nipah-infected population (magenta line) remains relatively stable, with minor fluctuations, suggesting a balance between infection transmission and recovery rates.
- The coinfected population (cyan line) exhibits an initial decline, followed by stabilization, indicating interactions between both infections and their combined impact on disease progression.
- The recovered population (yellow line) shows an increasing trend, signifying successful disease resolution and immunity development over time.

This visualization aids in understanding the complex interplay between multiple infections and their impact on population dynamics. The inclusion of fractional derivatives accounts for memory effects and non-Markovian transmission patterns, making the model more realistic for epidemiological studies. The trends observed in the figure validate the theoretical expectations of the model and provide insights into potential control strategies for

managing co-circulating infectious diseases.

Limitations of the Study: There was a lack of literatures above EBV/NIV coinfection and more compartments are added to coinfection model with parameter values.

7. Conclusion

In this study, we developed a comprehensive fractional-order mathematical model to analyze the co-infection dynamics of Ebola virus (EBOV) and Nipah virus (NIV). The incorporation of the Atangana-Baleanu fractional derivative has enabled a more nuanced representation of disease transmission processes by accounting for memory effects and non-local interactions, which are often neglected in traditional integer-order models.

Our key findings are summarized as follows:

- The use of fractional calculus, specifically the Atangana-Baleanu derivative, provides a flexible and accurate framework for modeling the complex interactions involved in EBOV and NIV co-infections, capturing effects that conventional models may overlook.
- Qualitative analyses utilizing fixed-point theorems have demonstrated the existence and uniqueness of solutions to the proposed model, confirming its mathematical robustness.
- Numerical simulations performed using the Adams-Bashforth-Moulton predictor-corrector method in MATLAB reveal that variations in the fractional order significantly influence disease transmission and co-infection dynamics. Notably, a fractional order of 0.99 exhibits behaviors distinct from the classical integer-order case, emphasizing the importance of memory effects.
- The model underscores the critical role of recovery rates and other parameters in shaping outbreak outcomes, highlighting potential avenues for targeted intervention strategies.

Despite these insights, limitations remain due to the scarcity of literature on EBOV/NIV co-infection and the need for further validation with empirical data. Future research directions include:

- Extending the model to incorporate additional compartments or co-infecting pathogens.
- Investigating long-term epidemiological implications across diverse ecological settings.
- Considering stochastic effects and real-world intervention measures to enhance model realism.

Overall, this work emphasizes the significance of fractional-order modeling in understanding complex infectious disease interactions. It provides valuable insights into disease dynamics and lays a foundation for developing effective control and prevention strategies against co-infections of high public health concern.

Data availability statement: The datasets utilized and/or analyzed during the current study can be obtained from the corresponding author upon reasonable request.

References

[1] S. Abbas, M. Ahmad, M. Nazar, Z. Ahmad, M. Amjad, H.A. Garalleh and A.Z. Jan, *Soret effect on MHD casson fluid over an accelerated plate with the help of constant proportional caputo fractional derivative,* ACS omega, **9**(9) (2024), 10220–10232.

[2] S. Abbas, M. Ahmad, M. Nazar, M. Amjad, H. Ali and A.Z. Jan, *Heat and mass transfer through a vertical channel for the Brinkman fluid using Prabhakar fractional derivative,* Appl. Thermal Eng., **232** (2023), 121065.

[3] S. Abbas, M. Nazar, S.F.F. Gillani, M. Naveed, M. Ahmad and Z.U. Nisa, *A CPC fractional model of the heat and mass transport mechanism in Carbon nanotubes with slip effects on velocity,* Modern Physics Letters B, **38**(13) (2024), 2450100.

[4] S. Abbas, M. Nazar, Z.U. Nisa, M. Amjad, S.M.E. Din and A.M. Alanzi, *Heat and mass transfer analysis of MHD Jeffrey fluid over a vertical plate with CPC fractional derivative*, Symmetry, **14**(12)(2022), 2491.

[5] S. Abbas, Z.U. Nisa, S.F.F. Gilani, M. Nazar, A.S.M. Metwally and A.Z. Jan, *Fractional Analysis of Magnetohydrodynamics Maxwell Flow Over an Inclined Plate with the Effect of Thermal Radiation*, Int. J. Theoretical Phys., **63**(5) (2024), 120.

[6] S. Abbas, Z.U. Nisa, M. Nazar, M. Amjad, H. Ali and A.Z. Jan, *Application of heat and mass transfer to convective flow of Casson fluids in a microchannel with CaputoFabrizio derivative approach,* Arabian J. Sci. Eng., **49**(1) (2024), 1275–1286.

[7] M. Abdelhakem, D. Baleanu, P. Agarwal and H. Moussa, *Approximating system of ordinary differential-algebraic equations via derivative of Legendre polynomials operational matrices,* Int. J. Modern Phys. C, **34**(3) (2023), 2350036.

[8] M. Abdelhakem, M. Fawzy, M. El-Kady and H. Moussa, *An efficient technique for approximated BVPs via the second derivative Legendre polynomials pseudo-Galerkin method: Certain types of applications,* Results in Phys., **43** (2022), 106067.

[9] M. Abdelhakem, M. Fawzy, M. El-Kady and H. Moussa, *Legendre polynomials second derivative tau method for solving Lane-Emden and Ricatti equations,* Appl. Math. Inf. Sci, **17**(3) (2023), 437–445.

[10] M. Abdelhakem and H. Moussa, *Pseudo-spectral matrices as a numerical tool for dealing BVPs, based on Legendre polynomials derivatives,* Alexandria Eng. J., **66** (2023), 301–313.

[11] P. Agarwal and R. Singh, *Modelling of transmission dynamics of Nipah virus (Niv): a fractional order approach*, Physica A: Stat. Mech. Appl., **547** (2020), 124243.

[12] S.O. Akindeinde, E. Okyere, A.O. Adewumi, R.S. Lebelo, O.O. Fabelurin and S.E. Moore, *Caputo fractional-order SEIRP model for COVID-19 Pandemic,* Alexandria Eng. J., **61**(1) (2022), 829–845.

[13] A.J. Ali, A.F. Abbas and M.A. Abdelhakem, *Comparative Analysis of Adams-Bashforth-Moulton and Runge-Kutta Methods for Solving Ordinary Differential Equations Using MATLAB,* Math. Model. Eng. Prob., **11**(3) (2024), 641–647.

[14] B.S.T. Alkahtani, *Chua's circuit model with AtanganaBaleanu derivative with fractional order,* Chaos, Solitons Fractals, **89** (2016), 547–551.

[15] J.K.K. Asamoah, E. Okyere, E. Yankson, A.A. Opoku, A. Adom-Konadu, E. Acheampong and Y.D. Arthur, *Non-fractional and fractional mathematical analysis and simulations for Q fever,* Chaos, Solitons Fractals, 156 (2022), 111821.

[16] M. Aslam, R. Murtaza, T. Abdeljawad, C.U. Rahman, A. Khan, H. Khan and H. Gulzar, *A fractional order HIV/AIDS epidemic model with Mittag-Leffler kernel,* Adv. Diff. Equ., **107** (2021), 1–15.

[17] T. Berge, J.S. Lubuma, C.M. Moremedi, N. Morris and R. Kondera-Shava, *A simple mathematical model for Ebola in Africa,* J. Biolog. Dyna., **11**(1) (2017), 42–74.

[18] M. Biava, C. Caglioti, L. Bordi, C. Castilletti, F. Colavita, S. Quartu and E. Lalle, *Detection of viral RNA in tissues following plasma clearance from an Ebola virus infected patient,* PLoS pathogens, **13**(1) (2017), e1006065.

[19] M.H.A. Biswas, *Model and control strategy of the deadly Nipah virus (NiV) infections in Bangladesh,* Res. Reviews in Biosci., **6** (12)(2012), 370–377.

[20] M.H. Biswas, *Optimal control of Nipah virus (NiV) infections: a Bangladesh scenario,* J. Pure Appl. Math.: Adv. Appl., **12**(1) (2014), 77–104.

[21] M.H.A. Biswas, M.M. Haque and G. Duvvuru, *A mathematical model for understanding the spread of nipah fever epidemic in Bangladesh,* In 2015 Int. Conference on Indus. Eng. Oper. Manag. (IEOM)IEEE, (2015), 1-8, IEEE.

[22] J. Brainard, K. Pond, L. Hooper, K. Edmunds and P. Hunter, *Presence and persistence of Ebola or Marburg virus in patients and survivors: a rapid systematic review,* PLoS Neglected Topical Diseases, **10**(2) (2016), e0004475.

[23] M. Caputo and M. Fabrizio, *A new definition of fractional derivative without singular kernel,* Progress in Fract. Diff. Appl., **1**(2) (2015), 73–85.

[24] CDC (Centers for Disease Control and Prevention), *Outbreak of Hendra-like virus-Malaysia and Singapore, 19981999,* MMWR Morb Mortal Wkly Rep., **48**(13) (1999), 265–269.

[25] P.J. Changdev, C. Dale and V. Chinchane, *On Dirichlet problem of Time-fractional Advection- Diffusion Equation,* J. fract. Calcu. Nonlinear Syst., **4**(2) (2023), 1–13.

[26] K.B. Chua, K.J. Goh, K.T. Wong, A. Kamarulzaman, P.S.K. Tan, T.G. Ksiazek and C.T. Tan, *Fatal encephalitis due to Nipah virus among pig-farmers in Malaysia,* The Lancet, **354**(9186) (1999), 1257–1259.

[27] G.F. Deen, N. Broutet, W. Xu, M. Knust, F.R. Sesay, S. McDonald and others, *Ebola RNA persistence in semen of Ebola virus disease survivorspreliminary report,* New England J. Medicine, **377**(15) (2015), 1428–1437.

[28] S. Khan, *Existence theory and stability analysis to a class of hybrid differential equations using confirmable fractal fractional derivative,* J. Fract. Calcu. Nonlinear Syst., **5**(1) (2024), 1–11.

[29] H. Khan, J.F. GómezAguilar, A. Alkhazzan and A. Khan, *A fractional order HIVTB coinfection model with nonsingular MittagLeffler Law. Mathematical Methods in the Applied Sciences,* **43**(6) (2020), 3786–3806.

[30] M.A. Khan, S. Ullah and M. Farooq, *A new fractional model for tuberculosis with relapse via AtanganaBaleanu derivative,* Chaos, Solitons Fract., **116** (2018), 227–238.

[31] K.A. Martins, P.B. Jahrling, S. Bavari and J.H. Kuhn, *Ebola virus disease candidate vaccines under evaluation in clinical trials,* Expert Review of Vaccines, **15**(9) (2016), 1101–1112.

[32] B. Mondal, A.A. Thirthar, N. Sk, M.A. Alqudah and T. Abdeljawad, *Complex dynamics in a two species system with CrowleyMartin response function: Role of cooperation, additional food and seasonal perturbations*, Math. Comput. Simul., **221** (2024), 415–434.

[33] H.S. Nita, D.T. Niketa, A.T. Foram and H.S. Moksha, *Control strategies for Nipah virus,* Int. J. Appl. Eng. Res., **13**(21) (2018), 15149–15163.

[34] E. Okyere, F.T. Oduro, S.K. Amponsah, I.K. Dontwi and N.K. Frempong, *Fractional order SIR model with constant population,* Br. J. Math. Comput. Sci., **14**(2) (2016), 1–12.

[35] M.A. Omoloye and S.O. Adewale, *Mathematical analysis of sensitive parameters on the dynamical transference of Ebola-malaria co-infections,* Int. J. Comput. Sci. Inform. Secu. (IJCSIS), **19**(7) (2021), 21-45.

[36] R. Pakhira, B. Mondal, A.A. Thirthar, M.A. Alqudah and T. Abdeljawad, *Developing a fuzzy logic-based carbon emission cost-incorporated inventory model with memory effects,* Ain Shams Eng. J., **15**(6) (2024), 102746.

[37] N.I. Paton, Y.S. Leo, S.R. Zaki, A.P. Auchus, K.E. Lee, A.E. Ling and T.G. Ksiazek, *Outbreak of Nipah-virus infection among abattoir workers in Singapore,* The Lancet, **354**(9186) (1999), 1253–1256.

[38] N.H. Shah, A.H. Suthar, F.A. Thakkar and M.H. Satia, *SEI model for transference of Nipah virus,* J. Math. Comput. Sci., **8**(6) (2018), 714-730.

[39] J. Singh, D. Kumar and D. Baleanu, *On the analysis of chemical kinetics system pertaining to a fractional derivative with Mittag-Leffler type kernel*, Chaos: An Interdisciplinary J. Nonlinear Sci., **27**(10) (2017), 103113.

[40] D. Sinha and A. Sinha, *Mathematical model of zoonotic nipah virus in south-east asia region,* Acta Sci. Micro., **2**(9) (2019), 82–89.

[41] A.A. Thirthar, S. Jawad, S.J. Majeed and K.S. Nisar, *Impact of wind flow and global warming in the dynamics of preypredator model,* Results Control Opti., **15** (2024), 100424.

[42] A.A. Thirthara, S. Jawadb, K. Shahc and T. Abdeljawadc, *How does media coverage affect a COVID-19 pandemic model with direct and indirect transmission?,* J. Math. Comput. Sci., **35** (2024), 169–181.

[43] P. Van den Driessche and J. Watmough, *Reproduction numbers and sub-threshold endemic equilibria for compartmental models of disease transmission,* Math. Biosci., **180**(1-2) (2002), 29–48.

[44] WHO Ebola Response Team, *Ebola virus disease among male and female persons in West Africa,* New England J. Medicine, **374**(1) (2016), 96–98.

[45] World Health Organization, *Ebola situation report30 March 2016,* WHO Emergency Situation Report, (2016), https://iris.who.int/handle/10665/204418.